

Level-broadening effects on the inelastic light-scattering spectrum due to coupled plasmon-phonon modes in δ -doped semiconductors

Guo-Qiang Hai, Nelson Studart, and Gilmar E. Marques

Departamento de Física, Universidade Federal de São Carlos, 13565-905 São Carlos, São Paulo, Brazil

(Received 6 January 1997; revised manuscript received 7 July 1997)

The Raman scattering intensity of δ -doped semiconductors is evaluated. The dynamical response of the multisubband two-dimensional electron system which is coupled to optical phonons is calculated within the random-phase approximation. Our calculation shows that both intrasubband and intersubband plasmon modes are strongly coupled to optical-phonon modes. Level broadening due to high impurity concentration modifies the inelastic light scattering spectrum significantly. However, a few scattering peaks corresponding to phonon-like modes can be observed even at large broadening. [S0163-1829(98)04304-5]

I. INTRODUCTION

Inelastic light (Raman) scattering has been used extensively to investigate novel aspects of the electronic structure and collective excitations in low-dimensional semiconductor systems.¹⁻⁵ In semiconductors with simple band extrema, collective excitations due to charge-density fluctuations and single-particle excitations related to spin density fluctuations have been observed.⁸ In polar semiconductors, the collective excitations due to charge-density fluctuations of the electron gas can be modified by their coupling to longitudinal-optical (LO) phonons as shown in light scattering experiments.^{1,6-8}

In δ -doped polar semiconductors, such as Si δ -doped GaAs, the plasmon-phonon coupling is quite pronounced and essentially important because the electron density is high and also because the energy separation between different subbands is close to the optical-phonon energy.⁹ The quasi-two-dimensional electron gas (Q2DEG) in a δ -doped semiconductor is formed by a highly doped impurity layer. Since the electrons share the same spatial region with the ionized donors, they are strongly scattered by the impurities. Consequently, the scattering reduces not only the electron mobility¹⁰ but also broadens the optical spectrum. The present work is intended to describe theoretically the light scattering spectrum due to coupled plasmon-phonon modes in the Si δ -doped GaAs system based on a self-consistent calculation of the subband structure and the dielectric many-body theory within the random-phase approximation (RPA). This paper stresses the broadening effects on the light spectrum and predicts the scattering peaks which can be detected experimentally. In Sec. II, we develop the dielectric formalism that is used to evaluate the plasmon-phonon spectrum and the inelastic light-scattering intensity. Section III is devoted to a discussion of the calculation results and in Sec. IV we summarize our main conclusions.

II. THEORETICAL FORMALISM

We have derived the inelastic light scattering cross section due to coupled plasmon-phonon modes in a *multisubband* Q2DEG embedded into a polar semiconductor. The inelastic light scattering intensity is related to the dynamical structure factor and can be written as

$$I(k_z, q, \omega) = \int dz \int dz' e^{-ik_z(z-z')} \times [-\text{Im}\{\epsilon_b(\omega)\chi(q, \omega, z, z')\}], \quad (1)$$

where k_z is the z component of wave vector of the incident light and q is the electron wave vector transfer in the xy plane. In Eq. (1), the polarization of the background polar semiconductor is modeled by a frequency-dependent dielectric function $\epsilon_b(\omega)$ determined by the longitudinal (ω_{LO}) and transversal (ω_{TO}) optical-phonon frequencies, with the following simplified form:

$$\epsilon_b(\omega) = 1 + \frac{\omega_{\text{TO}}^2 - \omega_{\text{LO}}^2}{\omega^2 - \omega_{\text{TO}}^2 + i\omega\eta}, \quad (2)$$

where we have introduced a phenomenological parameter η , to incorporate the phonon damping associated to possible defects in the crystalline structure.

The density-density correlation $\chi(q, \omega, z, z')$ of the Q2DEG is calculated as an expansion in single-particle wave functions $\psi_n(z)$, as

$$\chi(q, \omega, z, z') = \sum_{nn', mm'} \chi_{nn', mm'}(q, \omega) \psi_n(z) \times \psi_{n'}(z) \psi_m(z') \psi_{m'}(z'), \quad (3)$$

where $n, m = 1, 2, 3, \dots$, are the subband indices. The density-density correlation function $\chi_{nn', mm'}(q, \omega)$ is related to the dielectric function $\epsilon_{nn', mm'}(q, \omega)$ through the equation

$$\sum_{ll'} \epsilon_{ll', nn'}(q, \omega) \chi_{ll', mm'}(q, \omega) = \Pi_{nn'}(q, \omega) \delta_{nm} \delta_{n'm'}, \quad (4)$$

with the polarizability of the noninteracting electron gas given by

$$\Pi_{nn'}(q, \omega) = 2 \sum_k \frac{f_{n'}[E_{n'}(\vec{k} + \vec{q})] - f_n[E_n(\vec{k})]}{E_{n'}(\vec{k} + \vec{q}) - E_n(\vec{k}) + \hbar(\omega + i\gamma)}. \quad (5)$$

Here $f_n(E)$ is the Fermi-Dirac function, the electron energy is given by $E_n(k) = E_n + \hbar^2 k^2 / 2m^*$, m^* being the electron

effective mass, and γ is a phenomenological damping constant which takes into account the level broadening mainly induced by scattering of electrons by impurity centers. In the case $\gamma=0$, Stern¹¹ was the first to give an analytical expression for $\Pi_{nn'}(q, \omega)$. In general, the damping constant η for the phonon system is much smaller than the damping constant of electrons and, due to the high impurity concentration in the δ -doped system, we can safely take η as a positive infinitesimal in reliable calculations.

It is well known that the polarizabilities from both electron and phonon systems are additive in the RPA so that when both the electron-electron and the electron-phonon interactions are included we can write the total dielectric function as

$$\epsilon_{nn',mm'}(q, \omega) = \epsilon_b(\omega) \delta_{nm} \delta_{n'm'} - v_q F_{nn',mm'}(q) \Pi_{mm'}(q, \omega), \quad (6)$$

where $v_q = 2\pi e^2 / \epsilon_\infty q$ is the 2D Fourier transform of the bare electron-electron interaction, with ϵ_∞ being the high-frequency dielectric constant of the background. Finally $F_{nn',mm'}(q)$ is the Coulomb form factor which results from the spreading of the electron wave in the z direction and is given by¹⁰

$$F_{nn',mm'}(q) = \int_{-\infty}^{\infty} dz \psi_n(z) \psi_{n'}(z) \times \int_{-\infty}^{\infty} dz' \psi_m(z') \psi_{m'}(z') e^{-q|z-z'|}.$$

Note that by setting $\epsilon_b(\omega)=1$ in Eq. (6), the dielectric function of the Q2DEG in the RPA, without considering the electron-phonon interaction, is easily recovered.

Equations (1)–(6) describe the inelastic light scattering by charge density fluctuations of the coupled plasmon LO-phonon modes in a multisubband system. It is worth noticing that the light scattering intensity, given by Eq. (1), is proportional to the product of $\chi(q, \omega, z, z')$ and $\epsilon_b(\omega)$. As a consequence, one important feature is that the scattering intensity is zero at $\omega = \omega_{LO}$. This is a signature of a charge-density fluctuation mechanism because, at $\omega = \omega_{LO}$, there are no free-electron density fluctuations in the coupled plasmon LO-phonon system.

III. NUMERICAL RESULTS AND DISCUSSION

As in our previous works,^{9,10} we consider a Si δ -doped GaAs structure with a doping layer in the xy plane with thickness $W_D = 10$ Å. The background acceptor concentration in the sample is taken to be $n_A = 10^{15} \text{ cm}^{-3}$. In Fig. 1, the inelastic light intensity is indicated by solid curves, for different q 's, ranging from 10^4 to $1.4 \times 10^6 \text{ cm}^{-1}$, in the system where the electron density $N_e = 2 \times 10^{12} \text{ cm}^{-2}$ and $\gamma = 0.5 \text{ meV}$. In this situation, two subbands whose subband Fermi energies are $E_{F1} = 50.41 \text{ meV}$ and $E_{F2} = 11.24 \text{ meV}$ are occupied. The energy separations between subband pairs ($E_{nn'} = E_{n'} - E_n$) are $E_{12} = 39.17 \text{ meV}$, $E_{13} = 55.38 \text{ meV}$, and $E_{23} = 16.19 \text{ meV}$. In the calculation, we have included a third unoccupied subband. The thin solid curves show the scattering intensity due to plasmon modes of the Q2DEG,

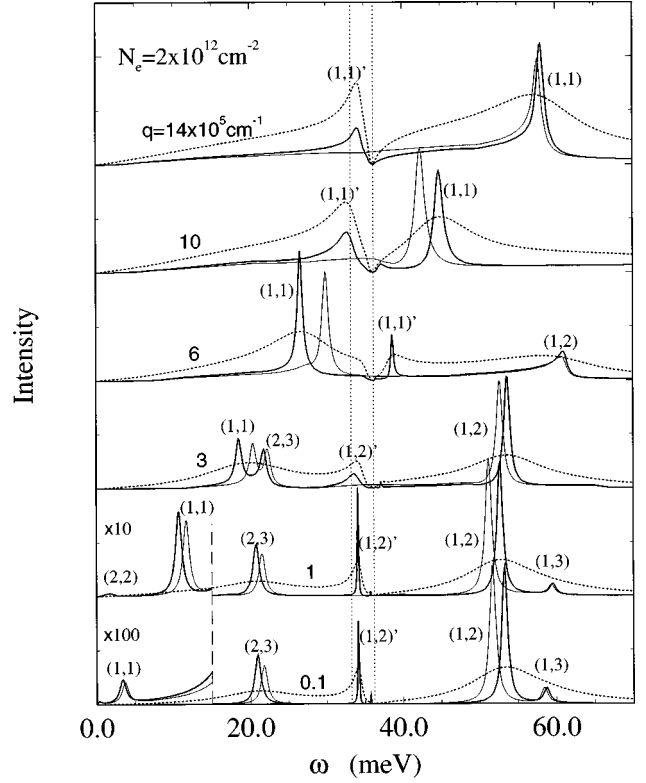


FIG. 1. The inelastic light scattering intensity due to plasmon (thin solid curves) and coupled plasmon-phonon modes at $q = 0.1, 1, 3, 6, 10,$ and $14 \times 10^5 \text{ cm}^{-1}$ in Si δ -doped GaAs with $N_e = 2 \times 10^{12} \text{ cm}^{-2}$. The thick solid and dotted curves indicate the results with $\gamma = 0.5$ and 6 meV , respectively. The scattering peaks due to different plasmon modes are labeled by (n, m) . Note the change in spectra scales: the intensity for $\gamma = 6 \text{ meV}$ is enlarged 3 times.

without phonons, and the thick solid curves are the results with the inclusion of the plasmon-phonon coupling. The vertical dotted lines indicate the frequencies of TO and LO phonons, $\hbar \omega_{LO} = 36.25 \text{ meV}$ and $\hbar \omega_{TO} = 33.29 \text{ meV}$, respectively.

The Raman spectrum in the absence of plasmon-phonon coupling exhibits a rich peak structure corresponding to excitation modes which are denoted by (n, m) . We can observe in the thin curves of Fig. 1, the peaks at small wave vectors related to the intrasubband modes (2,2) and (1,1), with very weak intensity, and the intersubband modes (2,3), (1,2), and (1,3). With increasing q , the peaks of the modes (2,2) and (1,3) disappear, while the peak corresponding to the (1,1) mode becomes pronounced and survives at large q . When the plasmon-phonon coupling is considered, a comparison of the two scattering spectra shows that the resonance frequencies below ω_{LO} are redshifted while those above ω_{LO} are blueshifted. More essentially, new coupled modes, which are denoted by $(n, m)'$, arise around ω_{LO} due to the plasmon-phonon coupling. At small q , we can see clearly a phononlike mode in the reststrahlen region of GaAs which comes from the phonon-coupling of the intersubband mode (1,2). At large q , the intrasubband mode (1,1) is strongly coupled to the phonons.

Now, we investigate the effect of the impurity scattering on the light spectrum, which is described by the broadening

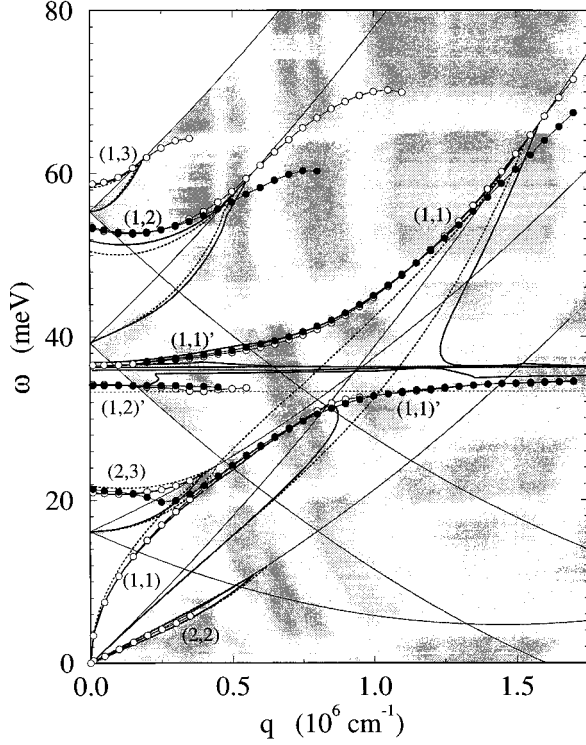


FIG. 2. The dispersion relations of the plasmon (thick dotted curves) and coupled plasmon-phonon (thick-solid curves) modes with $\gamma=0$ in the system of $N_e=2 \times 10^{12} \text{ cm}^{-2}$. The open and solid circles indicate the peak positions in the scattering spectrum due to coupled plasmon-phonon modes with $\gamma=0.5$ and 6 meV , respectively. The shaded area corresponds to the pair-excitation region (Landau damping).

width γ related to the electron subband quantum lifetime or the single-particle relaxation time. From our previous works,¹⁰ the subband quantum mobility varies from about $500 \text{ cm}^2/\text{Vs}$ (the lowest subband with energy of 24 meV) to $4000 \text{ cm}^2/\text{Vs}$ (the third subband with energy of 3 meV). The dotted curves in Fig. 1 represent the scattering intensity with $\gamma=6 \text{ meV}$. As expected, some of the peaks are merged. The scattering peak of the intrasubband mode $(1,1)'$ cannot be observed at small q . Also, those peaks corresponding to the intrasubband mode $(2,2)$ and to the intersubband $(1,3)$ disappear. However, the broadening does not affect considerably the phononlike modes, e.g., the peak $(1,2)'$ located at a little higher than ω_{TO} .

In order to clarify the scattering spectra, we have calculated the dispersion relations of the plasmon and coupled plasmon-phonon modes. For $\gamma=0$, the dispersion relation of the collective excitations can be obtained from⁹

$$\det|\epsilon_{nn',mm'}(q, \omega)|=0. \quad (7)$$

Figure 2 shows the plasmon dispersion (thick-dotted curves) and coupled plasmon-phonon modes (thick-solid curves) within the three-band model. The shaded area shows the single-particle spin-density excitation regime where $\text{Im} \Pi_{nn'} \neq 0$. It can be seen that the dispersion of the unperturbed plasmon modes $(1,1)$ and $(2,2)$ develops a loop in the $\omega-q$ plane. There are two frequencies, for a given q , but the lower branch is in the region where $\text{Im} \Pi_{n,n} \neq 0$ and the corresponding modes are strongly Landau damped. Due to the

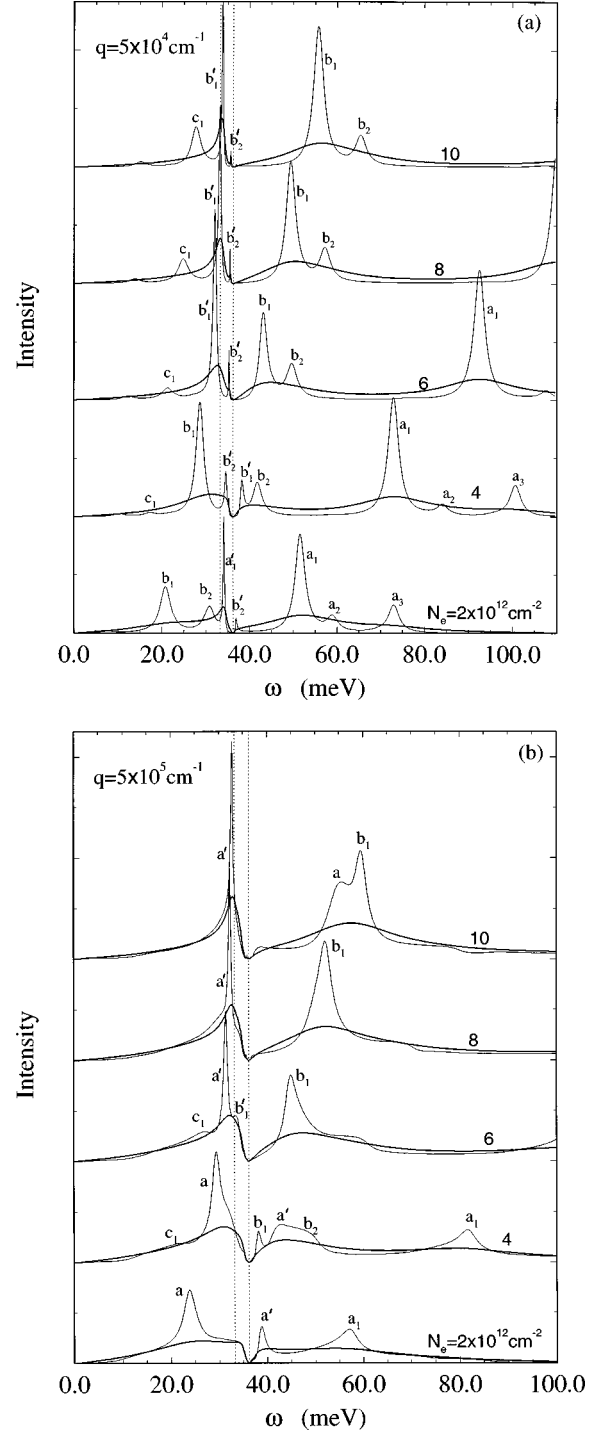


FIG. 3. The scattering spectra with $\gamma=1.5 \text{ meV}$ (thin curves) and $\gamma=10 \text{ meV}$ (thick curves) at (a) $q=5 \times 10^4 \text{ cm}^{-1}$ and (b) $q=5 \times 10^5 \text{ cm}^{-1}$ for the systems of different electron densities $N_e=2, 4, 6, 8,$ and $10 \times 10^{12} \text{ cm}^{-2}$. The scattering peaks due to different plasmon-phonon modes are labeled by a and a' ($1,1$); a_1 and a_1' ($1,2$); a_2 ($1,2$); a_3 ($1,4$); b_1 and b_1' ($2,3$); b_2 and b_2' ($2,4$); c_1 ($3,4$).

high electron density in the lowest subband, the unperturbed plasmon mode $(1,1)$ crosses over the LO-phonon frequency and the electron-phonon interaction leads to a splitting of this mode. The electron-phonon coupling also alters the intersubband mode $(1,2)$ by inducing a shift to higher frequency and another phononlike mode $(1,2)'$ arises between ω_{TO} and

ω_{LO} . The results obtained from the peak positions of the scattering spectrum with $\gamma=0.5$ and 6 meV are indicated by open and solid circles in Fig. 2, respectively. From the spectrum with $\gamma=0.5$ meV, we observe all the plasmon-phonon modes in the region where $\text{Im}\Pi_{n,m}=0$. From the above results, we conclude that (i) each mode (n,m) is Landau damped only in the region where $\text{Im}\Pi_{n,m}\neq 0$, (ii) the scattering peak coming from the intrasubband or intersubband mode vanishes slowly when it enters into its own single-particle continuum region, and (iii) the scattering intensity of the intrasubband modes is almost zero at small q and it increases with increasing q . Conversely, the intersubband modes exhibit the most intensity at small q , and it decreases with increasing q . For larger broadening, $\gamma=6$ meV, only three peaks can be observed at small q . These are related to the plasmonlike mode (2,3) and the coupled plasmon-phonon modes (1,2) and (1,2)'. At large q , these peaks disappear, but the intrasubband plasmon-phonon mode (1,1) becomes relevant. When we further increase γ , the calculated scattering spectrum remains similar to the structure for $\gamma=6$ meV.

Finally we discuss the electron density dependence of the light scattering spectrum for two wave vectors and two level-broadening widths. Figure 3 shows the Raman intensities at (a) $q=5\times 10^4$ cm⁻¹ and (b) $q=5\times 10^5$ cm⁻¹ for $N_e=2,4,6,8$, and 10×10^{12} cm⁻². The thin and thick curves are the results for $\gamma=1.5$ and $\gamma=10$ meV, respectively. With increasing electron density, the $n=2, 3$, and 4 subbands begin to be occupied at $N_e=0.93, 2.67$, and 8.33×10^{12} cm⁻², respectively. For $N_e=10^{13}$ cm⁻², four subbands are occupied. Then the contribution from the $n=4$ subband becomes prominent. In the calculation, we now have to consider a four-subband model. In Fig. 3(a), we see that the intrasubband scattering is very weak. For $\gamma=1.5$ meV, we can observe the scattering peaks due to the coupled intersubband plasmon-phonon modes labeled by $a_1: (1,2); a'_1: (1,2)'; a_2: (1,3); a_3: (1,4); b_1: (2,3); b'_1: (2,3)'; b_2: (2,4); b'_2: (2,4)';$ and $c_1: (3,4)$. The scattering due to intersubband modes from two adjacent subbands, such as (1,2) and (2,3), is significant. For high electron density $N_e=10^{13}$ cm⁻², the intersubband mode (3,4) also becomes pronounced. When $\gamma=10$ meV, most scattering peaks merge together and the scattering spectrum assumes a simple structure with a few broad peaks. However, the scattering peaks due to the phononlike modes, which are close to ω_{LO} , are not strongly affected. For $q=5\times 10^5$ cm⁻¹, the peak from the intrasub-

band mode (1,1) becomes the most important one, as is shown in Fig. 3(b). For the lower electron density $N_e=2\times 10^{12}$ cm⁻², we can see two peaks a and a' corresponding to the coupled intrasubband plasmon-phonon mode (1,1). For intermediate densities, the peak a from the (1,1) mode mixes with the peak b_1 from the (2,3) mode which dominates the scattering around this frequency. Also, the (2,3) and (3,4) modes merge into the lower peak (1,1). For the higher electron density, the peak below ω_{LO} is mainly due to the (1,1) mode, while the other one above ω_{LO} comes from the (2,3) mode.

IV. CONCLUSIONS

We have investigated the inelastic light scattering due to *coupled plasmon-phonon* modes in a *multisubband* Q2DEG realized in δ -doped semiconductors. Our study stressed the broadening effects (induced by impurity scattering) on the Raman spectrum and we have calculated the overall features of the spectrum which could be observed in realistic experimental situations. For small broadening, we have found a very rich structure in the light scattering spectrum. All the peaks due to different intra- and intersubband modes can be observed. At small q , the intersubband modes have the largest scattering strength. But the scattering due to the intrasubband modes of the lowest subband becomes very pronounced for large q . For large broadening widths, which corresponds closely to the experimental situation, most of the modes are strongly damped. Only a few scattering peaks clearly observable with a large full width at half maximum. However, the influence of the damping is not very pronounced for the phononlike modes which are close to the LO-phonon frequency. For $N_e=2\times 10^{12}$ cm⁻², the phononlike mode from the intersubband (1,2) can be seen clearly at small q . For large q , only the intrasubband mode (1,1) is relevant. For high electron density systems, the phonon-like mode from intersubband (2,3) becomes important at small q . We hope our results will provide useful information and stimulate further experimental study.⁸

ACKNOWLEDGMENTS

This work was partially sponsored by the Conselho Nacional de Desenvolvimento Científico e Tecnológico (CNPq) and the Fundação de Amparo à Pesquisa do Estado de São Paulo (FAPESP). G.Q.H. was supported by CNPq (Brazil).

¹G. Abstreiter, M. Cardona, and A. Pinczuk, in *Light Scattering in Solids IV*, edited by M. Cardona and G. Güntherodt (Springer-Verlag, Berlin, 1984), p. 36.

²J. K. Jain and S. Das Sarma, Phys. Rev. B **36**, 5949 (1987).

³X. Wu and S. E. Ulloa, Phys. Rev. B **48**, 14 407 (1993).

⁴L. Ioriatti, Phys. Rev. B **43**, 14 742 (1991); L. A. O. Nunes, L. Ioriatti, L. T. Florez, and J. P. Harbison, *ibid.* **47**, 13 011 (1993).

⁵V. Anjos, L. Ioriatti, and L. A. O. Nunes, Phys. Rev. B **49**, 7805 (1994).

⁶G. D. Mahan, *Many-Particle Physics* (Plenum, New York, 1981).

⁷E. H. Hwang and S. Das Sarma, Phys. Rev. B **52**, R8668 (1995).

⁸A. Mlayah, R. Carles, E. Bedel, and A. Muñoz-Yagüe, Appl. Phys. Lett. **62**, 2848 (1993); J. Appl. Phys. **74**, 1072 (1993).

⁹G.-Q. Hai, N. Studart, and G. E. Marques, Phys. Rev. B **55**, 1554 (1997).

¹⁰G.-Q. Hai, N. Studart, and F. M. Peeters, Phys. Rev. B **52**, 8363 (1995); G.-Q. Hai and N. Studart, *ibid.* **R2245**, (1995).

¹¹F. Stern, Phys. Rev. Lett. **18**, 546 (1967).